

Received August 24, 2019, accepted August 29, 2019, date of publication September 2, 2019, date of current version September 23, 2019.

Digital Object Identifier 10.1109/ACCESS.2019.2938991

# Scalability Analysis of Algebraic Graph-Based Multi-UAVs Formation Control

YU DING<sup>ID</sup>, XIANGKE WANG<sup>ID</sup>, (Senior Member, IEEE),

YIRUI CONG<sup>ID</sup>, (Member, IEEE), AND HUIMING LI

College of Intelligence Science and Technology, National University of Defense Technology, Changsha 410073, China

Corresponding author: Yirui Cong (congyirui11@nudt.edu.cn)

This work was supported by the National Natural Science Foundation of China under Grants 61973309 and 61801494.

**ABSTRACT** In multiple unmanned aerial vehicle (UAV) formation control systems, high scalability can guarantee the formation stability when UAVs join in or leave the system, and thus improves the robustness of the formation flight. This paper investigates the scalability problem for multi-UAV formation control with double-integrator dynamics. To be more specific, we focus how to build communication links with fixed control parameters such that the formation can always keep stable when adding/removing arbitrary number of UAVs. A bio-inspired method – Veteran Rule is proposed to solve this problem. Compared to the existing methods, our proposed method does not require to re-design or adaptively adjust the control parameters/gains for the changed Laplacian matrix. Furthermore, the convergence rate of the system under the Veteran Rule is analyzed. Surprisingly, the convergence rate of the system reaches the maximum value when all the in-degrees equal a particular value, rather than goes to infinity. Moreover, to guarantee the robustness of the formation system, we study the tolerance on undesired communication links (which break our proposed Veteran Rule). An upper bound for the coupling strength of the undesired communication links is provided by using Gershgorin circle theorem. Finally, simulation results corroborate the effectiveness of our results.

**INDEX TERMS** Double-integrator dynamics, formation control, optimal convergence rate, reverse edge, scalability, unmanned aerial vehicles, veteran rule.

## I. INTRODUCTION

### A. MOTIVATION

Nowadays, formation control of multiple unmanned aerial vehicles (UAVs) has attracted considerable attention due to not only its capability in executing complex missions, but also its wide range of applications in military and civil uses, such as target search and localization [1], contour mapping [2], surveillance and exploration [3], forest fire detection [4], etc.

The cooperative UAVs often fly in formation, and algebraic-graph-based formation control is one of two main techniques in supporting the formation flight, in which there are lots of articles about cooperative UAVs flying in formation [5], [6].<sup>1</sup> Since sometimes the number of a multi-UAV formation would change due to the mission requirements or the formation needs to fuse or divide, it is necessary to study the scalability problem in UAV formation control.

The associate editor coordinating the review of this manuscript and approving it for publication was Zhen Li.

<sup>1</sup>The other main technique in formation control is based on rigid graph [3].

Compared to the rigid-graph-based methods, even though the algebraic-graph-based control laws can be easily applied to a 3-dimensional formation and do not have the local minima problem [6], it is faced with the scalability issue. More specifically, when some UAVs attempt to join or leave the formation system, the Laplacian matrix of the communication topology will change accordingly. As a result, the original control parameters can be no longer effective (for those Laplacian matrix dependent methods, e.g., [1], [7]), or the parameters should be re-adjusted (for those adaptive consensus based methods, e.g., [8], [9]) due to the topology change. When the scale of the formation system gets very large, the amount of calculation will also increase rapidly, and thus the redesign of the control law becomes hard. The adaptive consensus method cannot perform well facing with large scale of the formation system, either, because it needs the whole system re-adjusts when new UAVs join in the system even though the original system has reached formation stability. To the best of our knowledge, the existing methods cannot handle the scale-changes properly without changing the control parameters,

and no closely related work has been devoted to the scalability problem. Thus, it is necessary to consider the formation scalability problem without changing the control parameters/gains in the whole formation system, i.e., with fixed individual control parameters.

Another important issue for the formation scalability is the convergence rate. Intuitively, the convergence rate may decrease as the number of UAVs changes; and a simple example is for single-integrator systems where the algebraic connectivity varies with the scale of the formation system. Hence, how to guarantee the convergence rate in the formation scalability problem is a meaningful and essential topic to study.

Furthermore, the robustness of scalability also plays a pivotal role in UAV formation systems. If the designed method is affected by some unexpected events, the corresponding tolerance should be analyzed.

## B. RELATED WORKS

In algebraic-graph-based formation control framework, consensus is a commonly used method, which means in a typical multi-agent system, each agent shares information only with its neighboring agents under a designed protocol while the whole group can coordinate to achieve a certain global behavior [10]. Consequently, this has resulted in tremendous amount of interest for this topic, and two pioneer papers on consensus problem are [11], [12]. Since then, the consensus problem has been extensively studied by numerous researchers and much progress has been made to the study of the conditions that a group of agents in a network reaching consensus, and a large variety of control strategies have been proposed and analyzed for various kinds of consensus problems. For example, [13] studied single-integrator multi-agent systems under time-invariant (time-varying) topology, and proposed a sufficient condition of reaching consensus that the topology (topology union) has a spanning tree. Afterwards, researchers began to study second-order systems and high-order systems. In [14], the authors proposed a sufficient condition of a second-order system reaching consensus, and then a necessary and sufficient condition was established in [15]. Reference [16] analyzed a general consensus protocol of multi-agent systems with double-integrator dynamics, and obtained the necessary and sufficient condition of general double-integrator consensus protocols. There is still a lot of literature and work on consensus, such as finite-time consensus problem [17], [18], system with linear and nonlinear dynamics [19], [20], etc. We recommend the survey papers [5], [6] to readers who are interested in the consensus problems for multi-agent systems.

However, as stated in Section I-A, the existing methods cannot handle the scale-changes properly:

Reference [21] proposed an interaction topology which is irrelevant to the magnitude of the couplings among agents. Reference [7] analyzed an observer-type consensus protocol based on relative output measurements between neighboring agents. However, the control laws in these studies rely on the

nonzero eigenvalue of the Laplacian matrix. Similarly, works like [14], [20] cannot solve the scale changing problem, either. This is because the design of the control law depends on the prior information of the whole Laplacian matrix to compute eigenvalues. This serious drawback requires that the control parameters must be redesigned due to the topology change.

For the fully distributed control laws, a notable method which can overcome the drawback from utilizing the spectrum information of Laplacian matrix is the adaptive consensus, in which the coupling among agents adjust according to the change of topology. Nevertheless, most of adaptive consensus studies are based on undirected communication topologies [9], [22]–[25]. Since the communication links are usually asymmetric, [8] then provided a general solution of linear consensus problem under directed communication topologies. The system can reach consensus using only the agent dynamics and the relative states of neighboring agents as long as the communication graph contains a directed spanning tree with the leader as the root node. However, when the initial consensus error is large, the coupling gain with the form of multiplying a new nonlinear function in the controller will increase rapidly, which may bring very big control input. Based on [8], [26] proposed a distributed adaptive observer to decouple the adaptive coupling gain from the input so that the magnitude of the control input would not be impacted by the high-gain coupling. But the shortcoming that the control parameters for other UAVs would be affected by the UAVs joining or leaving the system still exists, when the scale of the formation gets large, the whole system must adjust even only one new UAV joins in. To avoid this drawback, we propose our method inspired from pigeon flocks [27].

## C. OUR CONTRIBUTIONS

In this work, we study the scalability problem for the UAV formation governed by double-integrator dynamics under a directed communication topology. Our contributions are as listed as follows:

- i) A method inspired from pigeon formations to build interaction topology is proposed, and we call it the Veteran Rule. It is shown that when using the Veteran Rule, the system can always have the formation stability with system scalability, and the control parameter in each UAV is fixed. Moreover, comparing with redesigning methods our method is independent of any global information from the communication graph and do not demand a ground control station to send commands of switching control laws.
- ii) The convergence rate of the system under the Veteran Rule is analyzed. Intuitively, it seems that larger in-degrees lead to a higher convergence rate, since they represent stronger connection in a network. But surprisingly, the convergence rate of the system reaches the maximum value when all the in-degrees equal a particular value, rather than goes to infinity. Based on

this result, the Veteran Rule with optimal convergence rate is proposed.

- iii) To guarantee the robustness of the formation system, we study the tolerance on undesired communication links (which break our proposed Veteran Rule), i.e., reverse edges. An upper bound for the coupling strength of the reverse edges is provided by using Gershgorin circle theorem [28]. Based on this upper bound, we discuss how the reverse edges change the scalability of the formation system in different cases.

#### D. PAPER ORGANIZATION

The remainder of the paper is organised as follows. Section II gives the preliminaries of this paper, and it has three parts: Firstly, some basic concepts of graph theory are summarized in Section II-A. Secondly, the system model is given in Section II-B. Thirdly, Section II-C gives the problem description. In Section III, we propose the Veteran Rule to guarantee the formation scalability where a rigorous proof is given. Furthermore, convergence rate is analyzed and its optimal design is provided in Section IV. In Section V we give an upper bound of the strength of undesired communication links, and analyze the impact of these edges in topology on the system. In Section VI, simulation results corroborate the effectiveness of our methods. Finally, the concluding remarks are given in Section VII.

## II. SYSTEM MODEL AND PROBLEM DESCRIPTION

### A. BASIC CONCEPTS IN GRAPH THEORY

To present the problem description, some basic concepts in graph theory related to our work are briefly summarized in this subsection.

A directed graph  $\mathcal{G}$  can be described by a triple  $(\mathcal{V}, \mathcal{E}, \mathcal{W})$ , where  $\mathcal{V} = \{1, \dots, N\}$  is the node set, and  $\mathcal{E} \subseteq \mathcal{V} \times \mathcal{V}$  denotes the edge set, and  $\mathcal{W} = [w_{ij}] \in \mathbb{R}^{N \times N}$  with  $w_{ij} \geq 0$  represents the adjacency matrix such that  $(i, j) \in \mathcal{E}$  if and only if  $w_{ji} > 0$ . In this work, we assume  $\mathcal{G}$  is simple (i.e., with no self-edges), which means  $w_{ii} = 0$  for all  $i \in \mathcal{V}$ . The set of neighbors of node  $i$  is denoted by  $\mathcal{N}_i = \{j \in \mathcal{V} : (j, i) \in \mathcal{V}\}$ . The in-degree of the node  $i$  is defined by  $\deg_{\text{in}}(i) = \sum_{j \in \mathcal{N}_i} w_{ij}$ , and the degree matrix is  $\mathcal{D} = \text{diag}\{\deg_{\text{in}}(1), \dots, \deg_{\text{in}}(N)\}$ . With the adjacency matrix  $\mathcal{W}$  and the degree matrix  $\mathcal{D}$ , we can define the Laplacian matrix  $\mathcal{L}$  of  $\mathcal{G}$  by  $\mathcal{L} = \mathcal{D} - \mathcal{W}$ . A directed path from  $i$  to  $j$  is a sequence of ordered edges of the form  $(i, k_1), (k_1, k_2), \dots, (k_l, j)$ , and we say  $\mathcal{G}$  has a spanning tree if at least one node has a directed path to the other nodes. The following lemma gives some basic properties of the Laplacian matrix  $\mathcal{L}$ .

*Lemma 1 ([19]):* Let  $\mathcal{L} \in \mathbb{R}^{N \times N}$  be the Laplacian matrix of a directed graph  $\mathcal{G}$  and  $\mathbf{1}_N = [1, 1, \dots, 1]^T \in \mathbb{R}^N$ , then

- i)  $\mathcal{L}$  at least has a zero eigenvalue, and  $\mathbf{1}_N$  is the associated eigenvector, that is  $\mathcal{L}\mathbf{1}_N = 0$ ;
- ii) If  $\mathcal{G}$  has a spanning tree, then 0 is a simple eigenvalue of  $-\mathcal{L}$ , and all the other  $N - 1$  eigenvalues of  $-\mathcal{L}$  have negative real-parts.

*Definition 1 (Directed Acyclic Graph [29]):* If a directed graph has no directed cycles, that is to say, it is formed by a collection of vertices and directed edges, such that there is no path starting at some vertex  $v$  and follow a sequence of edges that loops back to  $v$  again, we call this kind of graph *directed acyclic graph (DAG)*.

In a DAG, we call the ordering of the vertices that the starting endpoint of every edge occurs earlier in the ordering than the ending endpoint of the edge the *topological ordering*. A DAG has a unique topological ordering if and only if it has a directed path containing all the vertices, in which case the ordering is the same as the order in which the vertices appear in the path. An edge is called a *reverse edge* if it is opposite to the topological ordering that the starting endpoint of the edge occurs later in the ordering than the ending endpoint [30].

### B. SYSTEM MODEL

Consider a multi-UAVs system of number  $N$  using local communications. A directed graph  $\mathcal{G}$  can be used to describe the communication topology of the formation system. More specifically, node  $i \in \mathcal{V}$  stands for the  $i^{\text{th}}$  UAV, and edge  $(i, j) \in \mathcal{E}$  represents the communication link from UAV  $i$  to UAV  $j$  whose strength is denoted by  $w_{ji}$ . All the UAVs move in  $d$ -dimensional space,  $d \in \{2, 3\}$ ,<sup>2</sup> and we let  $\xi_i(t) \in \mathbb{R}^d$  and  $\zeta_i(t) \in \mathbb{R}^d$  be the position and velocity states of UAV  $i$ , respectively. We assume the autopilot is properly designed such that the dynamics of each UAV  $i$  satisfies:

$$\begin{cases} \dot{\xi}_i = \zeta_i, \\ \dot{\zeta}_i = u_i, \end{cases} \quad (1)$$

where the input  $u_i \in \mathbb{R}^d$  is the acceleration of UAV  $i$  which can be timely controlled. In this work, we need all the UAVs achieve a given formation pattern and share the same speed. Here we consider the consensus-based formation controller as follows

$$u_i = - \sum_{j \in \mathcal{N}_i} w_{ij}[(\xi_i - \xi_j - \Delta_{ij}) + \gamma(\zeta_i - \zeta_j)], \quad (2)$$

where  $\Delta_{ij} = \Delta_i - \Delta_j$  denotes the desired relative position of UAV  $i$  w.r.t. UAV  $j$ ; and  $\Delta_i$  ( $\Delta_j$ ) is the offset of UAV  $i$  (UAV  $j$ ) determined by the formation pattern; and  $\gamma > 0$  is a parameter. By setting  $\xi = [\xi_1, \xi_2, \dots, \xi_N]$ ,  $\zeta = [\zeta_1, \zeta_2, \dots, \zeta_N]$ , and  $\hat{\xi} = [\xi_1 - \Delta_1, \xi_2 - \Delta_2, \dots, \xi_N - \Delta_N] =: \xi - \Delta$ , the closed-loop system with (1) and (2) can be written as

$$\begin{bmatrix} \dot{\hat{\xi}} \\ \dot{\zeta} \end{bmatrix} = \Gamma \otimes I_d \begin{bmatrix} \hat{\xi} \\ \zeta \end{bmatrix}, \quad (3)$$

where

$$\Gamma = \begin{pmatrix} 0 & I_{N \times N} \\ -\mathcal{L} & -\gamma \mathcal{L} \end{pmatrix}. \quad (4)$$

We say system (1) achieves formation stability, if  $\xi_i - \xi_j \rightarrow \Delta_{ij}$  and  $\zeta_i - \zeta_j \rightarrow 0$  as  $t \rightarrow \infty$ . Note that system (3) simplifies the analysis of the formation stability defined in Remark 1.

<sup>2</sup> $d = 2$  means UAVs fly in a plane, while  $d = 3$  implies UAVs fly in a  $R^3$  space

*Remark 1 (Formation Stability):* System (3) achieving consensus is equivalent to achieving the formation stability. Thus, for all  $i \in \{1, \dots, N\}$ , the following equation holds

$$\lim_{t \rightarrow \infty} \left\| \begin{bmatrix} \hat{\xi} \\ \zeta \end{bmatrix} - c(t) \otimes \mathbf{1}_N \right\| = 0, \quad (5)$$

where  $c(t)$  is called the consensus state trajectory or consensus function [19].

With  $c(t)$ , we can define the formation error as

$$\delta(t) = \begin{bmatrix} \xi - \Delta \\ \zeta \end{bmatrix} - c(t) \otimes \mathbf{1}_N, \quad (6)$$

whose asymptotic convergence is equivalent to that in (5).

Next, we define the convergence rate of formation error as follows.

*Definition 2 (Convergence Rate):* The convergence rate of the formation error  $\delta(t)$  is the largest exponent  $\beta^*$  to exponentially bound  $\|\delta(t)\|$  [31], i.e.,

$$\beta^* = \max\{\beta < 0 : \|\delta(t)\| \leq \alpha(\|\delta(0)\|) e^{\beta t}\}, \quad (7)$$

where  $\alpha(\cdot)$  is a class  $\mathcal{K}$  function [32].

### C. PROBLEM DESCRIPTION

In this paper, we study the scalability problem for formation control that without changing control parameter  $\gamma$ , how to design the communication links as well as their strengths such that:

- i) The formation system is still stable after adding new UAVs, i.e., the system has scalability (see Problem 1);
- ii) The convergence rate of the formation error is maximized (see Problem 3);

Note that the scalability does not intrinsically hold in formation systems. When adding new UAVs, the same control parameter  $\gamma$  cannot always maintain the formation stability, if the communication links and their strengths are not properly designed. The following proposition gives the necessary and sufficient condition for the formation stability, which well explains why  $\gamma$  is correlated to the scale of formation system.

*Proposition 1 ([33]):* Assume that the interaction topology  $\mathcal{G}$  has a spanning tree. Let  $\mu_i$  denote the  $i^{\text{th}}$  eigenvalue of  $-\mathcal{L}$ .  $\text{Re}(\mu_i) = p_i$  and  $\text{Im}(\mu_i) = q_i$  are the real and imaginary parts of  $\mu_i$ , respectively. Then the system (1) achieves formation stability (see Definition 1) if and if only

$$\gamma > \max_{2 \leq i \leq N} \frac{q_i}{\sqrt{-p_i} |\mu_i|}. \quad (8)$$

From Proposition 1, we can see that a formation stable  $\gamma$  is constrained by the communication links and their strengths (through the Laplacian matrix  $\mathcal{L}$ ). Consider a formation system with  $N$  UAVs which has reached formation stability. Assume  $M$  new UAVs join in this system, and they will build communication links to the original  $N$  UAVs, which leads the Laplacian matrix  $\mathcal{L}$  extends to  $N + M$  dimensions. New elements of the new Laplacian matrix will change the original  $N$  eigenvalues, and also bring new  $M$  eigenvalues.

This means the originally satisfied condition (8) is fragile after adding new UAVs. Similarly, consider the number of UAVs in the original formation is  $N + M$ . When  $M$  UAVs quit the formation, even if the new communication topology has a spanning tree, the originally established inequality (8) can hardly hold. Thus, it is necessary to study the scalability problem in formation control systems, which is formally defined in Problem 1 and Problem 2.

*Problem 1:* Assume the formation system with  $N \geq 1$  UAVs is formation stable (see Definition 1). After adding arbitrary  $M \geq 1$  UAVs but without changing  $\gamma$ , how to build new communication links to these  $M$  UAVs such that the new formation system with  $N + M$  UAVs is still formation stable?

*Problem 2:* Assume the formation system with  $M + N$  UAVs is formation stable, how to guarantee formation stability when  $M$  UAVs quit from the original  $N + M$  UAVs without changing  $\gamma$ ?

In Section III, we will provide the solutions to Problem 1 and Problem 2.

## III. THE VETERAN RULE AND FORMATION SCALABILITY

### A. THE VETERAN RULE

In nature we often see pigeons flying in a flock. Even though sometimes several separated individuals will join or leave the flock, the flock still maintains its formation and keeps stable. So analyzing the behavior model of pigeons may give us some inspiration to solve the formation scalability problem. In this section, we will show a interaction basic rule that we found among pigeons, which we call it “Veteran Rule”. According to this rule, we build an interaction topology, and show that with this kind of topology the system can always achieve formation stability and possess the property of scalability.

Through the study of pigeon flocks, we have a conclusion that experienced pigeons tend to fly in front of the flock, while unexperienced pigeons tend to fly in latter of the flock [34]. Based on this, we call the pigeon with more navigation experience in a pair the “local leader” and the other with less experience the “local follower”. It is found that the local leader always tends to take the position of front while the local follower tends to fly in latter of the local leader [35]. Through visual information, local followers can respond (usually copy and imitate) to the behavior of the local leader [27], thus local followers will be able to accomplish their homing or migration [36]. However, the local followers are in local leaders’ blind spots so that whatever they do, their local leaders cannot perceive their behavior, thus will not make any response [37]. Thus we can say the information transfer is only from local leaders to local followers, in other words, the information transfer is only from experienced individuals to unexperienced pigeons. We call this rule “Veteran Rule”, that the information transfer is only from experienced individuals to unexperienced individuals, or we say unexperienced individuals only obtain unidirectional information from experienced individuals (see Fig. 1).

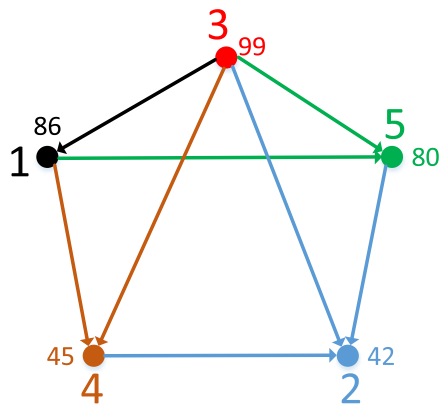


**FIGURE 1.** Nodes in the topology above represent pigeon individual 1 – 5. The experience of each pigeon is quantified as 86, 42, 99, 45 and 80, respectively. The Veteran Rule means the information only transfer from experienced individuals to unexperienced individuals, and thus a topology example shown above is formed.

### B. FORMATION SCALABILITY

For UAVs, we define a  $Q$  value  $Q(i)$  similar to the experience of pigeons in the flock for each UAV  $i$  in the system: i) the  $Q$  value of each UAV is unique, and ii) the  $Q$  values of any two UAVs are comparable.

*Theorem 1:* Assume that the communication topology  $\mathcal{G}$  has a spanning tree, when using the Veteran Rule (i.e. information only flows from high value UAVs to low value UAVs), the system always achieves formation stability, and can solve the scalability problem (i.e., Problem 1 and Problem 2).

*Proof:* This proof is divided into two steps. In the first step, we prove that the communication topology built according to the Veteran Rule corresponds to a directed acyclic graph. Then in the second step, we prove the formation stability and the scalability.

Firstly, to prove the graph is a directed acyclic graph, we only need to prove for any node pair of nodes  $i$  and  $j$  with  $Q(i) > Q(j)$ , and there is never a directed path from  $j$  back to  $i$ . Since the communication topology has a spanning tree, the former statement is obvious according to the Veteran Rule. Next we will prove there is never a directed path from  $j$  to  $i$  by contradiction. Assume there is a directed path from  $j$  to  $i$  that passes  $j, j_1, \dots, j_k, i$ , which implies  $Q(j) > Q(j_1) > \dots > Q(j_k) > Q(i)$ . This is contradicted with  $Q(i) > Q(j)$ . Thus there is never a directed path from  $j$  back to  $i$  for any two given nodes  $i$  and  $j$ , which means the graph is a directed acyclic graph according to Definition 1.

Secondly, we will show the system achieve formation stability regardless of the system scale. Denote the elementary matrix that exchanges the  $i$ th row and  $j$ th row as  $P_{ij}$ . For any adjacency matrix corresponding to a directed acyclic graph  $W$ , denote  $U = P_{i_11}P_{i_22}\cdots P_{i_NN}$ , where  $i_1, i_2, \dots, i_N$  are the nodes of the system whose  $Q$  values are ranked in a decreasing order. By applying the transformation  $W^* = U^{-1}WU$  to the adjacency matrix, the nodes are ranked in the topological order, which implies the adjacency matrix of the system satisfies for any  $i < j$ , for  $Q(i) > Q(j)$ ,  $w_{ij}^* = 0$ . So the adjacency matrix and the Laplacian matrix of the

system is a lower triangular matrix.<sup>3</sup> The eigenvalues of the Laplacian matrix  $\mu_i$  is a real negative number. By this time  $q_i = \text{Im}(\mu_i) = 0$ , which implies the necessary and sufficient condition (8) becomes  $\gamma > 0$ . Thus the system achieves formation stability. For  $N$  can be an arbitrary number, the conclusion holds when the number of the formation is  $N + M$ . Similarly, for  $M$  UAVs quiting the formation of  $N + M$  UAVs, the system can still achieve formation stability if all the UAVs follow the Veteran Rule. So as long as the new UAVs comply the Veteran Rule that if low  $Q$  value UAVs only receive information from high  $Q$  value UAVs in the communication topology, the system can always reach formation stability and possesses the property of scalability. ■

With Theorem 1, we can solve Problem 1 and Problem 2. When new UAVs join in the formation, they can build connections according to the Veteran Rule and receive information from agents whose  $Q$  values are higher than themselves'. When an UAV  $i$  quits the formation, the original links from UAV  $i$  to UAV  $j$  (generalize for all the UAVs receive information from  $i$ ) breaks which may cause the spanning tree disintegrates in the topology. Thus when UAV  $i$  quit, UAV  $j$  looks for UAVs with higher  $Q$  values than itself's and builds connections to receive information from upper agents. In this way, the spanning tree in the topology  $\mathcal{G}$  can be guaranteed by ensuring each UAV (except for the UAV with the highest  $Q$  value) has a neighbor whose  $Q$  value higher than itself's as its local leader, the formation maintains formation stability.<sup>4</sup>

*Remark 2:* One may ask what if a new UAV does not find a higher  $Q$  value upper UAV in its neighborhood? In this case, it is unavoidable to build reverse edges which breaks the Veteran Rule, since otherwise the communication topology would have no spanning tree. Therefore, we need to analyze the robustness of the Veteran Rule w.r.t. reverse edges, which is discussed in Section V.

Although the stability problem of scaled formation is solved by the Veteran Rule, it seems that the increasing number of UAVs in the formation may decrease the convergence rate of the system, which rises Problem 3.

*Problem 3:* Based on Problem 1 and Problem 2, how to design the strengths  $w_{ij}$  for communication links so that the convergence rate  $\beta^*$  (see Definition 2) is maximized?

In Section VI-B, we analyse the convergence rate of the system and propose the solution to Problem 3.

### IV. CONVERGENCE RATE ANALYSIS

Convergence rate is an important performance index of a system. In this section we consider the convergence rate maximization problem (i.e., Problem 3) under the Veteran Rule. In other words, the formation control system keeps scalable, while maximizes the convergence rate.

<sup>3</sup>Another method to prove the Laplacian matrix corresponding to a directed acyclic graph can be transformed into a lower triangular matrix is shown in [21].

<sup>4</sup>It is worth noting that we do not care about the process of obtaining  $Q$ , but how to realize the scalability of the formation with  $Q$  values.

Intuitively speaking, it seems that larger in-degrees lead to a higher convergence rate, since they represent stronger connection in a network. However, this is not true. In this section, we show that the in-degrees are not the larger the better, and the maximum convergence turns out to be achieved when all the in-degrees equal a particular value.

To analyze the convergence rate of the system, we should focus on the mode of the system dynamics. According to

$$\det(\lambda I_N + \mathcal{L}) = \prod_{i=1}^N (\lambda - \mu_i), \quad (9)$$

we can calculate the eigenvalues of  $\Gamma$  (as shown in (4)) by

$$\begin{aligned} \det(\lambda I_{2N} - \Gamma) &= \det(\lambda^2 I_N + (1 + \gamma\lambda)\mathcal{L}) \\ &= \prod_{i=1}^N (\lambda^2 - \gamma\mu_i\lambda - \mu_i) = 0. \end{aligned}$$

Solve the equation and we get

$$\lambda_{i\pm} = \frac{\gamma\mu_i \pm \sqrt{\gamma^2\mu_i^2 + 4\mu_i}}{2} \quad (10)$$

as the eigenvalue of  $\Gamma$  corresponding to  $\mu_i$ . By analyzing the mode of the system (3), it is straightforward that  $\beta^* = \max_{2 \leq i \leq N} \text{Re}(\lambda_{i\pm})$ . We should notice that  $\lambda_i$  are only correlated with  $\gamma$  and  $\mu_i$ , where  $\gamma$  is a constant we do not want to change, and  $\mu_i$  varies from 0 to  $-\infty$ . Since  $\text{Re}(\lambda_i)$  are negative real numbers, the maximum convergence rate implies  $\min \beta^*(\mu_i) \quad i = 2, 3, \dots, N$ , i.e.,  $\min \max_{2 \leq i \leq N} \text{Re}(\lambda_{i\pm})$ . So Problem 3 transforms into: When  $\beta^*$  reaches its minimum when  $\mu_i \quad i = 2, 3, \dots, N$  varies?

*Theorem 2:* The convergence rate of the system is maximized when the in-degree of every node equals to  $\frac{4}{\gamma^2}$ .

*Proof:* For the order of the nodes does not affect eigenvalues of  $\Gamma$  and the size relation of in-degrees, thus for simplify denoting the subscript and without loss of generality, we assume the agents are ranked in the topological order, and the in-degrees of nodes  $d_i$  satisfy  $d_2 \leq d_3 \leq \dots \leq d_N$ . Since the Laplacian matrix  $\mathcal{L}$  is a lower triangular matrix, the in-degree of each node is  $d_i = -\mu_i$ . Denote  $\lambda_{i+} = \frac{\gamma\mu_i + \sqrt{\gamma^2\mu_i^2 + 4\mu_i}}{2}$  and  $\lambda_{i-} = \frac{\gamma\mu_i - \sqrt{\gamma^2\mu_i^2 + 4\mu_i}}{2}$ . The convergence rate of the system correlate with  $\max_{2 \leq i \leq N} \text{Re}(\lambda_i)$ , and for each  $\mu_i$ , the corresponding  $\lambda_{i\pm}$  always have  $\text{Re}(\lambda_{i-}) \leq \text{Re}(\lambda_{i+})$ . So when talking about the convergence rate, we just need to care about all the  $\lambda_{i+}$ . To analyse the variation of  $\lambda_i$ , we draw the parameter root locus of  $\lambda$  when  $\mu$  varies from 0 to  $-\infty$  (see Fig. 2). Since  $|\mu_2| \leq |\mu_3| \leq \dots \leq |\mu_N|$ , we know that  $\lambda_{i+}(\mu_i) \quad i = 3, 4, \dots, N$  runs in front of  $\lambda_{2+}(\mu_2)$  along the root locus. Through the root locus we know that (see Fig. 2)  $\lambda_- \rightarrow -\infty$  as  $\mu \rightarrow -\infty$ , and  $\lambda_+ \rightarrow -\frac{1}{\gamma}$  as  $\mu \rightarrow -\infty$ .  $\text{Re}(\lambda)$  reaches its minimum at the right endpoint of the circle (noted with a triangle in Fig. 2), moving forward along the root locus,  $\lambda_+$  runs on the real axis from  $-\frac{2}{\gamma}$  to  $-\frac{1}{\gamma}$ . Thus we

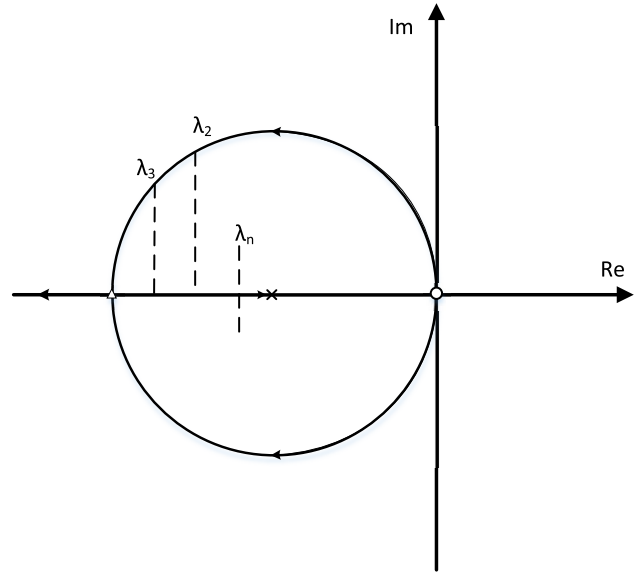


**FIGURE 2.** The root of polynomial  $\lambda^2 - \lambda\mu\gamma - \mu$  with  $\mu$  varying from 0 to  $-\infty$ . The root locus of eigenvalues  $\lambda$  starts from the origin. At the very beginning,  $\text{Re}(\lambda)$  decreases along the circle  $(x + \frac{1}{\gamma})^2 + y^2 = \frac{1}{\gamma^2}$  to  $-\frac{2}{\gamma}$ . As  $\mu$  continues increasing,  $\lambda_{i\pm}$  lie on the negative part of the real axis:  $\lambda_-$  tends to  $-\infty$ , while  $\lambda_+$  tends to  $-\frac{1}{\gamma}$ . The eigenvalues of the Laplacian matrix  $\mu_i$  have an order of  $|\mu_2| \leq |\mu_3| \leq \dots \leq |\mu_N|$ , so  $\lambda_{i+}(\mu_i) \quad i = 3, 4, \dots, N$  runs in front of  $\lambda_{2+}(\mu_2)$  along the root locus. Thus, we have  $\min |\text{Re}(\lambda_{\mu_{i+}})| = \min \{|\text{Re}(\lambda_{\mu_{2+}})|, |\text{Re}(\lambda_{\mu_{N+}})|\}$ .

have

$$\beta^* = \max \text{Re}(\lambda_{\mu_{i+}}) = \max \{|\text{Re}(\lambda_{\mu_{2+}})|, |\text{Re}(\lambda_{\mu_{N+}})|\}. \quad (11)$$

When  $\text{Re}(\lambda_{\mu_{2+}})$ ,  $\text{Re}(\lambda_{\mu_{N+}})$  simultaneously reaches their minimum,  $\beta^*$  reaches its global minimum. Thus the optimal situation is all the  $\lambda_{i+}$  lie on the right endpoint of the circle, which implies  $\mu_{i_2} = \mu_{i_N} = -\frac{4}{\gamma^2}$ . By this time,  $\beta^* = \lambda_{i_2} = \lambda_{i_N} = -\frac{2}{\gamma}$ . Thus when the in-degree  $d_i = \sum_{j=1}^N w_{ij} = \frac{4}{\gamma^2} \quad i = 2, 3, \dots, N$ ,  $\beta^*$  reaches its minimum  $-\frac{2}{\gamma}$ . ■

*Remark 3:* If a small  $\gamma$  is chosen, the corresponding coefficient of the system exponent  $\frac{2}{\gamma}$  increases and thus the system achieves consensus with a higher convergence rate.

One may ask with the input form  $u_i = -\sum_{j=1}^N w_{ij}[(\xi_i - \xi_j - \delta_{ij}) + \gamma(t)(\zeta_i - \zeta_j)] \quad i = 1, 2, \dots, N$ , it seems like a contradiction when  $\gamma$  tends to 0, that the gain decreases while the convergence rate of the system increases. Since the in-degree of the node is  $\sum_{j=1}^N w_{ij}$ ,  $w_{ij}$  can be considered as a linear function of the in-degree of the node,  $w_{ij} = \frac{4}{k\gamma^2} k \in R^+$  (each  $w_{ij}$  has a linear growth with the increase of the in-degree), then the gain of the system is  $w_{ij}\gamma = \frac{4}{k\gamma}$ . Thus with the decrease of  $\gamma$ , the gain of the input is actually increasing, which coincides with a faster convergence rate. Similarly if a large  $\gamma$  is chosen,  $\frac{4}{\gamma^2}$  may be very small, at this time  $w_{ij}$  should also be small to adapt the magnitude of  $\frac{4}{\gamma^2}$ . Since the maximum absolute value of

minimal-real-part eigenvalue is  $\frac{2}{\gamma}$ , under this circumstance the optimal convergence rate would be reduced.

## V. THE REVERSE EDGE

In pigeon flocks, high level members seldom look backward to form a cycle in their interaction topology. However, sometimes the lower level pigeons may detect some new food or be threatened by some predators. Then, the direction switching information will influence the upper level ones, which constitutes some additional reverse links [30]. It is mathematically easy to prove that adding temporary reverse edges is equivalent to changing the initial value of the system, which does not change the tendency that the system converges in pigeon flocks. However, sometimes in a UAV formation some reverse edges may exist all the time. Practically there are many factors such as spatial distance or some unknown disturbances that constrains the UAVs in the system building connections completely coinciding with the Veteran Rule. Or as we mentioned in Remark 2 some UAVs have to build connections with other agents to guarantee the spanning tree in topology so that information does not exactly transfer from high  $Q$  value agents to low  $Q$  value agents. Therefore, we need the topology have a tolerance of adding reverse edges so that the system still reaches consensus. So a fundamental problem is to find an upper bound for the coupling strength of the reverse edges (see Problem 4). Without loss of generality, in this section we discuss the problem under the assumption that the nodes are ranked in the topological order, and we define a concept *the reverse range*, in which reverse connections between these nodes are permitted.

**Definition 3 (The Reverse Range):** The reverse range is a set whose elements are the vertices with reverse edges from the minimal topological order number to the maximal topological order number.

**Problem 4:** Assume the reverse range is from  $i$  to  $k$ , and the elements in the reverse range matrix are  $w_{ls}$  ( $i \leq l, s \leq k$ ). Under what conditions of  $w_{ls}$ , the formation stability of the system is not affected by reverse edges in topology? Next we will give an upper bound of the tolerance of the coupling strength of the reverse edge.

We denote  $\mathcal{L}'$  as the new Laplacian matrix with reverse edges, and the submatrix of  $\mathcal{L}'$  formed from rows  $i, \dots, k$  and column  $i, \dots, k$  as the reverse range matrix  $A$  (see Fig. 3). For each agent  $l$  ( $i \leq l \leq k$ ) in the reverse range, let  $A_{1l} = \sum_{s=1}^{i-1} w_{ls}$  denote the summation of coupling strengths with agents from 1 to  $i-1$ , i.e., the agents with highest  $i-1$   $Q$  values.  $A_{2l} = \sum_{s=i}^l w_{ls}$  stands for the summation of coupling strengths of edges satisfying the Veteran Rule in the reverse range matrix  $A$  in Fig. 3, and  $A_{3l} = \sum_{s=l+1}^k w_{ls}$  presents the summation of coupling strength of reverse edges on agent  $l$ . The following theorem upper bounds the summation of the coupling strengths of all possible reverse edges in the reverse range, which provides a solution to Problem 4. Note that

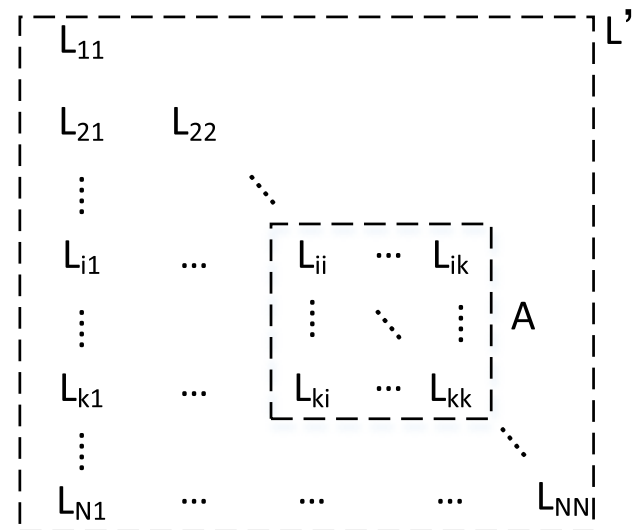


**FIGURE 3.** The minimal topological order number of nodes with reverse edges is  $i$ , while the maximal number is  $k$ , the reverse range of the topology is  $\{i, i+1, \dots, k\}$ . The submatrix of  $\mathcal{L}'$  from  $L_{ii}$  to  $L_{kk}$  is called the reverse range matrix, denoted as  $A$ .

$A_{2l} + A_{3l}$  presents the summation of the coupling strength between  $l$  and other agents in the reverse range.

**Theorem 3:** For each agent  $l$ , the following two conditions guarantee the formation stability:

- i) When  $A_{1l} \geq \frac{1}{\gamma^2}$ ,  $A_{3l}$  can be arbitrarily large;
- ii) When  $A_{1l} < \frac{1}{\gamma^2}$ ,  $A_{2l} + A_{3l} < \frac{1}{2}A_{1l}(\frac{1}{(1-\gamma\sqrt{A_{1l}})^2} - 1)$ .

*Proof:* After adding the reverse edge, the Laplacian matrix turns to the form of Fig. 3, denoted as  $\mathcal{L}'$ . Note that except for submatrix  $A$ , the residant of  $\mathcal{L}'$  is the same as the original  $\mathcal{L}$ . Thus we just need to consider eigenvalues of  $-A$  [denoted as  $z_l$  ( $i \leq l \leq k-1$ )].

When  $z_l$  all satisfy (8), the system achieves system stability. To analyze the eigenvalues of matrix  $-A$ , we use the Gershgorin Theorem [28] to matrix  $-A$ . The Gershgorin discs are

$$|z_l - (-L'_{ll})| < \sum_{s=i}^l |-L_{ls}| + \sum_{s=l+1}^k |-L_{ls}| \quad (i \leq l \leq k-1), \quad (12)$$

where  $L_{ll} = -\mu_l + A_{3l}$ ,  $L_{ls} = -w_{ls}$ . The proof is now divided into two steps. In the first step, we prove that when the curve  $q^2 = -\frac{\gamma^2 p^3}{1+\gamma^2 p}$  is separate from all the Gershgorin discs, such that the formation stability can be achieved. In the second step, we obtain the upper bound of  $A_{3l}$  that guarantees the curve is separate from all the discs.

According to the Gershgorin Theorem, all the eigenvalues of  $-L'$  lie in the union of the Gershgorin discs. When the curve  $q^2 = -\frac{\gamma^2 p^3}{1+\gamma^2 p}$  is separate from all the Gershgorin disks, all the eigenvalues  $z_l$  satisfy  $q_l^2(1 + \gamma^2 p_l) < -\gamma^2 p_l^3$ , which is equivalent to  $\gamma > \frac{q_l}{\sqrt{-p_l|z_l|}}$ . From Proposition 1, the system achieves formation stability. Then, the formation stability problem becomes: when the curve  $q^2 = -\frac{\gamma^2 p^3}{1+\gamma^2 p}$  is separate from all the Gershgorin discs (see Fig. 4).

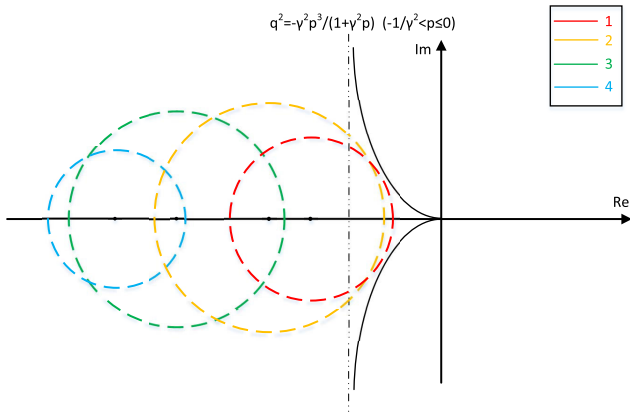


**FIGURE 4.** The eigenvalues of  $-L'$ ,  $z_l$  ( $i \leq l \leq k-1$ ) lie in the union of Gershgorin discs. Disc 1 and 2 correspond to case ii) while disc 3 and 4 correspond to case i). When the curve  $q^2 = -\frac{\gamma^2 p^3}{1+\gamma^2 p}$  is separate from all the Gershgorin circles,  $z_l$  satisfy (8), the system achieves formation stability.

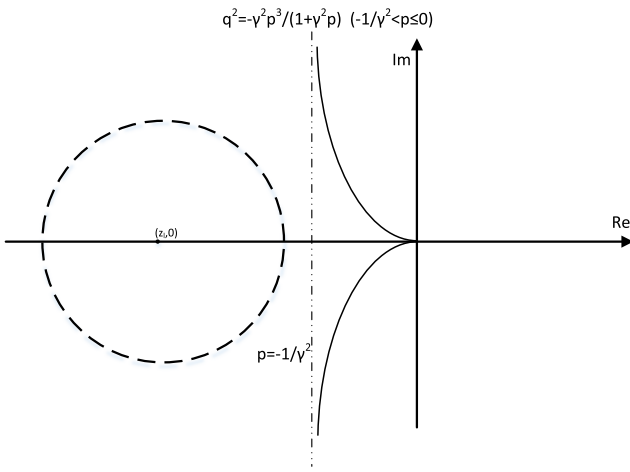


**FIGURE 5.** When  $-\sum_{s=1}^{i-1} w_{ls} < -\frac{1}{\gamma^2}$ , the endpoint of the circle is on the left side of  $(-\frac{1}{\gamma^2}, 0)$ , the eigenvalue  $z_l$  lying in this kind of discs satisfies  $p_l < -\frac{1}{\gamma^2} < -\frac{q_l^2}{\gamma^2 |z_l|}$ , i.e.  $y > \frac{q_l}{\sqrt{-p_l |z_l|}}$ ; thus the magnitude of the radius has no effects on the formation stability.

For i),  $-A_{1l} = -\sum_{s=1}^{i-1} w_{ls} \leq -\frac{1}{\gamma^2}$ , the left endpoint of this type of disc never lies on the right side of  $(-\frac{1}{\gamma^2}, 0)$ , as shown in Fig. 5. Thus the eigenvalue  $z_l$  lying in this kind of discs satisfies  $p_l < -\frac{1}{\gamma^2} < -\frac{q_l^2}{\gamma^2 |z_l|}$ , which satisfies condition (8). In this case, the radius of the Gershgorin disc can be infinite, and the curve will never intersect this kind of discs, which implies  $A_{3l}$  can reach infinity.

For ii),  $-A_{1l} = -\sum_{s=1}^{i-1} w_{ls} > -\frac{1}{\gamma^2}$ , the left endpoint of the disc is on the right side of  $(-\frac{1}{\gamma^2}, 0)$ , as shown in Fig. 6. To guarantee curve  $q^2 = -\frac{\gamma^2 p^3}{1+\gamma^2 p}$  has no intersections with the Gershgorin discs, the radius of the circle cannot be unboundedly large. As shown in Fig. 6, the critical situation is the curve is tangent to the disc.

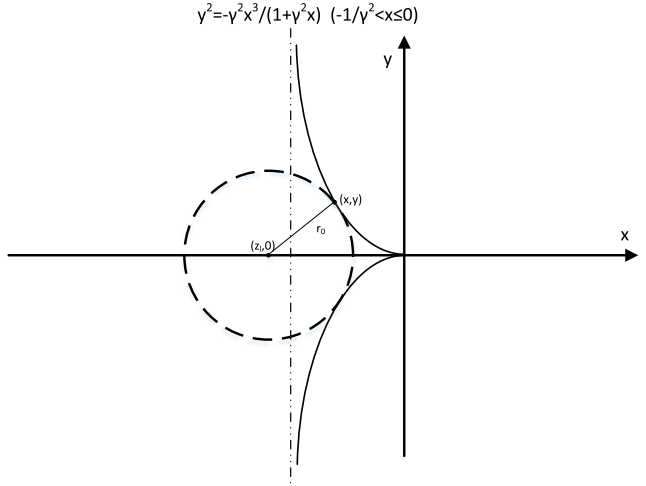


**FIGURE 6.** The critical situation is the curve  $y^2 = \frac{-\gamma^2 x^3}{1+\gamma^2 x}$  ( $-\frac{1}{\gamma^2} < x \leq 0$ ) has two tangent points to the circle  $(x - z_l)^2 + y^2 = r_0^2$  at the point  $(x, y)$ ,  $r_0$  is the upper bound of the radius which correlate with  $A_{3l}$ .

The center of the circle is  $(z_l, 0)$ , and the tangent point is  $(x, y)$ , and the critical radius of the circle is  $r_0$ , (as shown in Fig. 6). Under this circumstances, the tangent point satisfies

$$y'_x \cdot \frac{y}{x - z_l} = -1. \quad (13)$$

Taking the derivatives at both sides of the equation  $y^2 = \frac{-\gamma^2 x^3}{1+\gamma^2 x}$  w.r.t.  $x$ , we have

$$2y \cdot y'_x = \frac{-\gamma^2 [3x^2(1 + \gamma^2 x) - \gamma^2 x^3]}{(1 + \gamma^2 x)^2}. \quad (14)$$

With (13) and (14), we get an equation w.r.t.  $x$ :

$$(x - z_l)(1 + \gamma^2 x)^2 = \gamma^2 [3x^2(1 + \gamma^2 x) - \gamma^2 x^3], \quad (15)$$

which has two roots  $x_1 = -\frac{1}{\gamma^2} - \frac{1}{\gamma^2 \sqrt{1-2\gamma^2 z_l}}$  and  $x_2 = -\frac{1}{\gamma^2} + \frac{1}{\gamma^2 \sqrt{1-2\gamma^2 z_l}}$ . For  $x_1 < -\frac{1}{\gamma^2}$ , it contradicts  $-\frac{1}{\gamma^2} < x \leq 0$ ; thus the x-coordinate of the tangent point is  $x = x_2 = -\frac{1}{\gamma^2} + \frac{1}{\gamma^2 \sqrt{1-2\gamma^2 z_l}}$ . Then, we obtain the critical radius of the disc

$$\begin{aligned} r_0^2 &= (x - z_l)^2 + y^2 = \left(\frac{1}{\gamma^2} - \frac{1}{\gamma^2 \sqrt{1-2\gamma^2 z_l}} + z_l\right)^2 \\ &\quad - \frac{\gamma^2(-\frac{1}{\gamma^2} + \frac{1}{\gamma^2 \sqrt{1-2\gamma^2 z_l}})^3}{1 + \gamma^2(-\frac{1}{\gamma^2} + \frac{1}{\gamma^2 \sqrt{1-2\gamma^2 z_l}})}. \end{aligned}$$

Since radius of the Gershgorin disc is  $\sum_{s=i}^l |w_{ls}| + \sum_{s=l+1}^k |w_{ls}| = A_{2l} + A_{3l}$ , under the critical circumstance we have

$$\begin{aligned} (A_{2l} + A_{3l})^2 &= \left(\frac{1}{\gamma^2} - \frac{1}{\gamma^2 \sqrt{1-2\gamma^2 z_l}} + z_l\right)^2 \\ &\quad - \frac{\gamma^2(-\frac{1}{\gamma^2} + \frac{1}{\gamma^2 \sqrt{1-2\gamma^2 z_l}})^3}{1 + \gamma^2(-\frac{1}{\gamma^2} + \frac{1}{\gamma^2 \sqrt{1-2\gamma^2 z_l}})}, \end{aligned}$$

where  $z_l = \mu_l - A_{3l}$ . Define  $\sqrt{1 - 2\gamma^2 z_l}$  as  $m$ , then we have  $A_{3l} = \mu_l + \frac{m^2 - 1}{2\gamma^2}$ . Simplifying the equation we obtain

$$(1 - \gamma^2 A_{1l})m^2 - 2m + 1 + \gamma^2 A_{1l} + \gamma^4 A_{1l}^2 = 0 \quad (16)$$

Solving the equation we obtain two solutions

$$m_1 = \frac{1}{1 + \gamma\sqrt{A_{1l}}} + \gamma\sqrt{A_{1l}}, m_2 = \frac{1}{1 - \gamma\sqrt{A_{1l}}} - \gamma\sqrt{A_{1l}}.$$

As  $\frac{\gamma^2 A_{1l}}{(1 + \gamma\sqrt{A_{1l}})^2} \leq \gamma^2 A_{1l}$ , we have  $m_1^2 \leq 1 + 2\gamma^2 A_{1l}$ , which contradicts  $m^2 = 1 - 2\gamma^2 z_l = 1 + 2\gamma^2 A_{1l} + 2\gamma^2 A_{2l} + 2\gamma^2 A_{3l}$ . Therefore  $m_1$  is discarded, and  $m_2$  is the unique solution of (16). That is to say, when

$$A_{3l} \leq \frac{m_2^2 - 1}{2\gamma^2} - A_{1l} - A_{2l} = \frac{1}{2} A_{1l} \left( \frac{1}{(1 - \gamma\sqrt{A_{1l}})^2} - 1 \right) - A_{2l}, \quad (17)$$

the system will always achieve formation stability. ■

From the proof above we know that the larger  $A_{1l}$  is, the better robustness  $A_{3l}$  will get. When  $A_{1l}$  is large enough, i.e.  $A_{1l} \geq \frac{1}{\gamma^2}$ ,  $A_{2l} + A_{3l}$  can be arbitrarily large, which gives no constraints when agent  $l$  builds connections with agents in the reverse range. Thus,  $A_{3l}$  can go to infinity, which means the reverse edges can have infinite coupling strength in this case. When  $A_{1l} < \frac{1}{\gamma^2}$ ,  $A_{2l}$  has to be considered when building reverse connections to guarantee the stability.

*Remark 4:* The appearance of the reverse edge changes the scalability of the system. Three situations are considered when new agents join in the system.

- i) The new agent  $N + 1$  owns a  $Q$  value higher than the agent  $i$ . In this case, it can be relabeled with a number  $l_1$ , where  $l_1 < i$ , and the new element  $w_{il_1}$  would appear. So  $\sum_{s=1}^{i-1} w_{ls}$  would increase, and the reverse edge is still in the stable region, the system still achieves formation stability. On the contrary, the quitting of agents with  $Q$  values higher than agent  $i$  will decrease  $\sum_{s=1}^{i-1} w_{ls}$  and the upper bound of the coupling of reverse edge, the existing reverse edges may exceed the upper bound, the system may become unstable.
- ii) The new UAV joins in the reverse range. In this case, the new agent  $N + 1$  can be relabeled according to the  $Q$  value order with a number  $l_1$ , where  $i < l_1 < k$ . New elements of the Laplacian matrix appear on the  $l^{\text{th}}$  row,  $l_1 < l \leq k$ , which increases  $\sum_{s=l}^i w_{ls}$  and decreases the upper bound  $\frac{1}{2} A_{1l} \left[ \frac{1}{(1 - \gamma\sqrt{A_{1l}})^2} - 1 \right] - A_{2l}$ . Thus the existing reverse edges may exceed the upper bound, the system may become unstable. Moreover, the  $l_1$  Gershgorin disc may intersect the curve  $q^2 = \frac{-\gamma^2 p^3}{1 + \gamma^2 p}$  so that some eigenvalues may enter the unstable region through the  $l_1^{\text{th}}$  circle, and the formation stability of the system would be affected. Opposite to joining the system, when agents in the reverse range quit the formation, the upper

bound would increase and the stability would not be affected as long as the spanning tree is guaranteed.

- iii) The new agent owns a  $Q$  value lower than the agent  $k$ . This situation is simple, for the joining or quitting of the new agent apparently affect neither  $A_{1l}$  nor  $A_{2l}$ , thus the system still achieves formation stability.

*Remark 5:* The upper bound we mentioned above is a sufficient but not necessary condition, for it just guarantees no eigenvalue lies in the unstable region. For the eigenvalue is a uncertain point in the Gershgorin disc (without computing with global information), the intersection of the curve  $q^2 = \frac{-\gamma^2 p^3}{1 + \gamma^2 p}$  and the Gershgorin circle does not mean the eigenvalues of  $L'$  cannot satisfy (8). Thus it is not a necessary condition to the formation stability of the system.

*Remark 6:* When the reverse edge appears in agents  $i$  and  $i + 1$ , i.e., the reverse range is 2, the coupling strength of reverse edge can also go to infinity. Assume the agent  $l + 1$  builds reverse edge with agent  $l$ , the form of reverse range is  $\begin{pmatrix} L_{ll} & -w_{ll+1} \\ -w_{l+1l} & L_{l+1l+1} \end{pmatrix}$ . Since it is a  $2 \times 2$  strictly diagonally dominant matrix, according to Vieta theorem, the eigenvalues of reverse range are two real negative numbers, who satisfy  $\gamma > \frac{q_l}{\sqrt{-p_l |z_l|}} = 0$ , thus the coupling of reverse edge  $w_{ll+1}$  does not affect the stability of the system.

## VI. SIMULATION

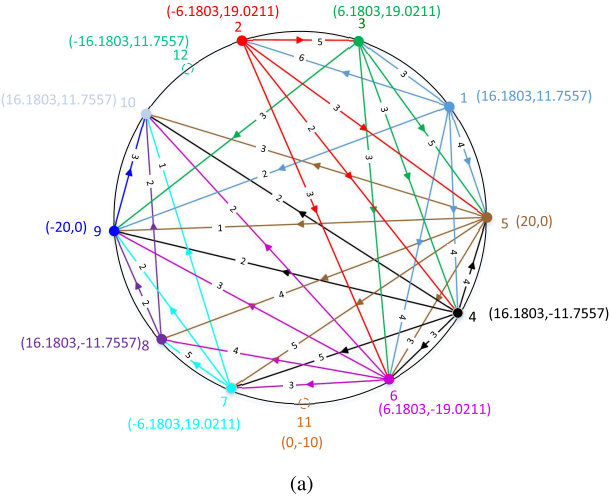
This section contains three subsections, in which UAVs are modeled with a double-integrator model. In Section VI-A, we corroborate the effectiveness of our proposed Veteran Rule in formation scalability, where the formation systems with 12 and 600 UAVs are considered, respectively. In Section VI-B, our theoretical results in the optimal convergence rate are verified. In Section VI-C, reverse edge related simulations are presented to illustrate the effectiveness of our results.

### A. THE VETERAN RULE

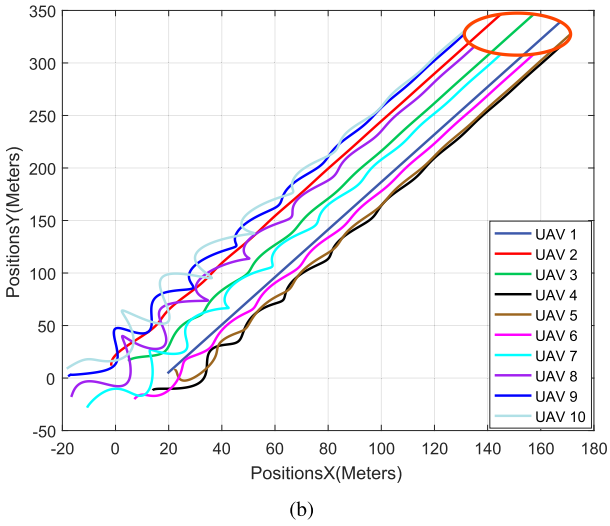
To demonstrate the effectiveness of the Veteran Rule in UAV formation, a 10 UAV formation system with 2 new joining UAVs is considered. The adjacency matrix of the 10 UAV system is

$$W = \begin{bmatrix} 0 & 0 & 0 & 0 & 0 & 0 & 0 & 0 & 0 & 0 \\ 6 & 0 & 0 & 0 & 0 & 0 & 0 & 0 & 0 & 0 \\ 3 & 5 & 0 & 0 & 0 & 0 & 0 & 0 & 0 & 0 \\ 3 & 2 & 3 & 0 & 0 & 0 & 0 & 0 & 0 & 0 \\ 4 & 3 & 5 & 4 & 0 & 0 & 0 & 0 & 0 & 0 \\ 4 & 3 & 3 & 3 & 3 & 0 & 0 & 0 & 0 & 0 \\ 0 & 0 & 0 & 5 & 5 & 3 & 0 & 0 & 0 & 0 \\ 0 & 0 & 0 & 0 & 4 & 4 & 5 & 0 & 0 & 0 \\ 2 & 0 & 3 & 2 & 1 & 3 & 2 & 2 & 0 & 0 \\ 0 & 0 & 0 & 2 & 3 & 2 & 1 & 2 & 3 & 0 \end{bmatrix}, \quad (18)$$

and the control parameter is  $\gamma = 0.1$ . Assume the UAVs are ranked in the topological order of their  $Q$  values, which



(a)



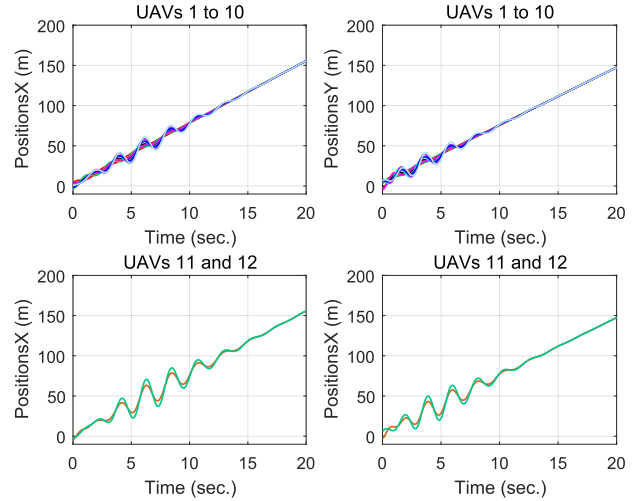
(b)

**FIGURE 7.** The UAVs are ranked in the reverse order of their  $Q$  values,  $Q(1) > Q(2) > \dots > Q(10)$ , and the 10 UAVs system finally goes forward in a shape of circle. (a) Communication topology and formation pattern of the 10 UAV formation system (e.g.,  $(5, 20)$  means  $\Delta_5 = [5, 20]^T$ ), where we also label UAVs 11 and 12 (new UAVs to join the formation system) using dashed circles. (b) 10 UAVs achieve formation stability and form the expected circle pattern.

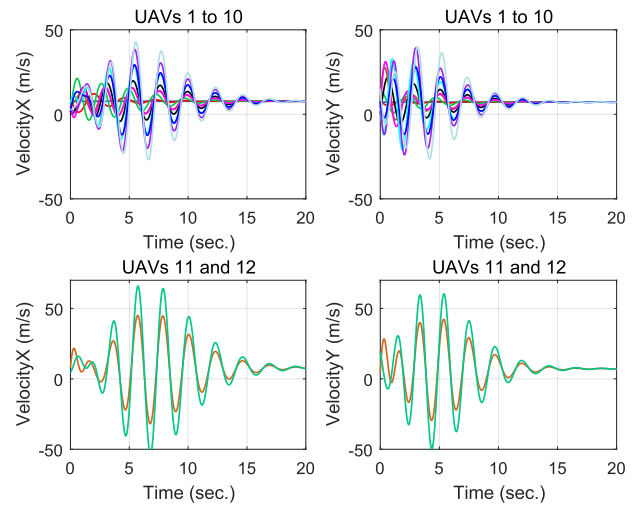
implies  $Q(1) > Q(2) > \dots > Q(10)$ . The communication topology as well as the formation pattern of the system are shown in Fig. 7(a) and the 10 UAV system finally forms a circle pattern [see Fig. 7(b)].

Without loss of generality, we assume the two joining UAVs'  $Q$  values satisfy  $Q(12) < Q(11) < Q(10)$ , and the relative positions for UAVs 11 and 12 are  $\Delta_{11} = [0, -10]^T$  and  $\Delta_{12} = [-16.1803, 11.7557]^T$ , respectively [see Fig. 7(a)]. When using the Veteran Rule, the added edges in the topology are  $w_{11,2} = 3, w_{11,5} = 2, w_{11,6} = 3, w_{11,7} = 2, w_{11,9} = 3, w_{11,10} = 2, w_{12,7} = 2, w_{12,8} = 3$ , and  $w_{12,9} = 4$ . By Theorem 1, the system will finally achieve formation stability, and the response curves of  $\hat{\xi}$  and  $\zeta$  are as shown in Fig. 8(a) and Fig. 8(b), respectively.

Next we will give an example as a comparison that the new two UAVs build connections without the Veteran Rule. Besides the edges coincide with the Veteran Rule we



(a)

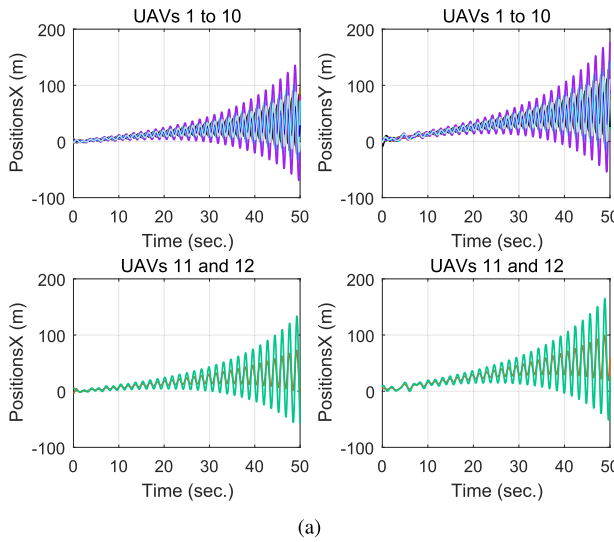


(b)

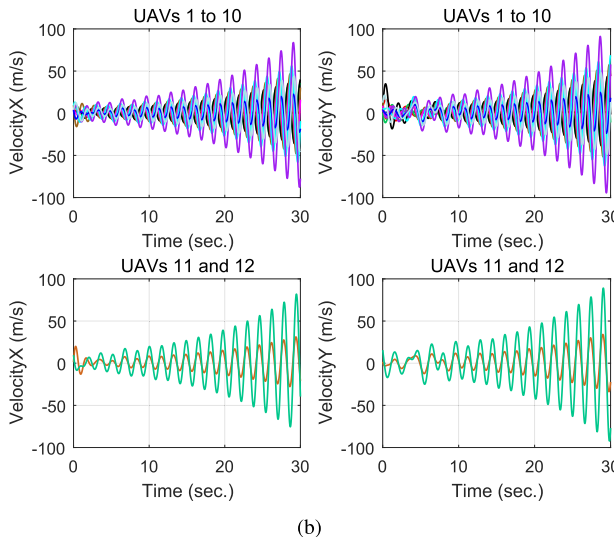
**FIGURE 8.** Two new UAVs using the Veteran Rule join in the flock. After a short period of oscillation, the system reaches formation stability. (a) Position curves of the formation system; (b) Velocity curves of the formation system.

mentioned above, some more reverse edges are also added in the topology:  $w_{3,11} = 1, w_{4,11} = 2, w_{6,11} = 1, w_{8,11} = 1, w_{9,11} = 1, w_{10,11} = 2, w_{4,12} = 2, w_{7,12} = 2, w_{8,12} = 1, w_{9,12} = 2, w_{10,12} = 1$ , and  $w_{11,12} = 6$ . One of the eigenvalues of the new Laplacian matrix is  $\mu = -12.8136 \pm 5.5.328i, p = \text{Re}(\mu) = -12.8136, q = \text{Im}(\mu) = 5.5328, \frac{q}{\sqrt{|p||\mu|}} = 0.111$  which does not satisfy the necessary and sufficient condition given in Proposition 1. Thus the system cannot achieve formation stability, and the curves of  $\hat{\xi}$  and  $\zeta$  are shown in Fig. 9(a) and Fig. 9(b), respectively. This simulation verifies our conclusion that building connection regardless of the Veteran Rule may lead formation instability.

Another of our simulation in Fig. 10 further shows the effectiveness of the Veteran Rule that the system still achieves formation stability when the scale of the formation goes very large (with 600 UAVs forming a cube in  $R^3$  space).



(a)



(b)

**FIGURE 9.** Two new UAVs join in the system without using the Veteran Rule, and the system diverges. (a) Position response of the system; (b) Velocity response of the system.

### B. CONVERGENCE RATE

We use a similar setting in the  $10+2$  UAV formation example in Section VI-A to analyze the optimal convergence rate, and the only difference is the control parameter  $\gamma = 0.5$ . From Theorem 2, we know that the optimal in-degree for each UAV is  $\frac{4}{\gamma^2} = 16$ . We assume all the 10 UAVs in the original formation system chose this optimal in-degree, and see how the convergence rate  $\beta^*$  changes when UAVs 11 and 12 vary their in-degrees from 10 to 20 (see Fig. 11). From Fig. 11 we can observe that the convergence rate reaches its maximum value when the in-degrees of UAVs 11 and 12 are equal to  $\frac{4}{\gamma^2} = 16$ , which corroborates the result in Theorem 2.

### C. THE REVERSE EDGE

Recall the example two UAVs joining in the 10 UAV formation system given in Section VI-A. The reverse range is from 3 to 12, and let  $\tau$  represent the upper bound of reverse

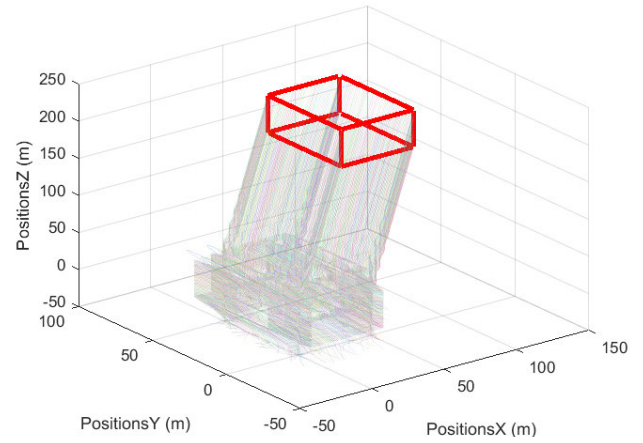


**FIGURE 10.** A formation system with 600 UAVs using the Veteran Rule, where the formation pattern is a  $50 \times 50 \times 50$  cube in  $R^3$  space.

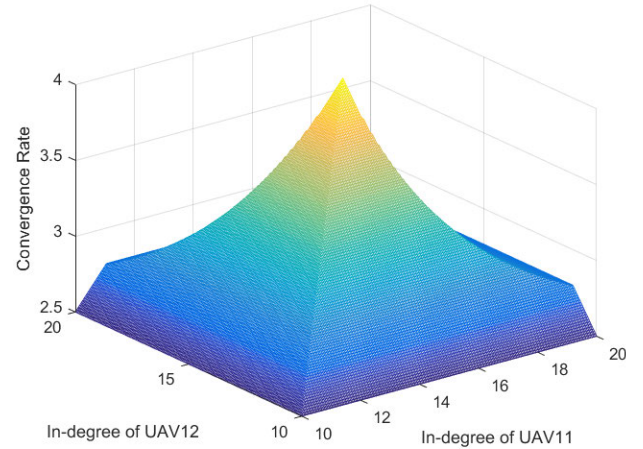


**FIGURE 11.** The in-degrees of the original 10 UAVs are all  $\frac{4}{\gamma^2} = 16$ . As the in-degree of UAV11 and UAV12 vary,  $\min_{2 \leq i \leq N} |\operatorname{Re}(\lambda_i)|$ , which measures the convergence rate of the system, is shown above. When the in-degrees of UAV 11 and 12 equal 16,  $\min_{2 \leq i \leq N} |\operatorname{Re}(\lambda_i)|$  reaches its maximum.

edges. Using the conclusion we obtain in Section V, we get  $\tau_3 = 3.78$ ,  $\tau_4 = -1.35$ ,  $\tau_5 = -6.02$ ,  $\tau_6 = -6.02$ ,  $\tau_7 = -13$ ,  $\tau_8 = -13$ ,  $\tau_9 = -12.64$ ,  $\tau_{10} = -13$ ,  $\tau_{11} = -11.31$ . We can find that when the coupling of reverse edges exceeds the upper bound, the system becomes unstable and no more maintains formation stability.

Next we will show that when the strengthen of reverse edges are smaller than the reverse upper bound we gave in Section V, the system can achieve formation stability. Consider a system with 20 UAVs,  $\gamma = 0.05$ . The reverse range of the system is from 6 to 10, with the reverse edges  $w_{6,10} = 2.772$  and  $w_{8,10} = 0.1734$ . For  $A_{1l}$  we have  $A_{1,6} = 12$ ,  $A_{1,7} = 13$ ,  $A_{1,8} = 13$ ,  $A_{1,9} = 14$ ,  $A_{1,10} = 13$ , and for  $A_{2l}$  we have  $A_{2,6} = 0$ ,  $A_{2,7} = 3$ ,  $A_{2,8} = 3$ ,  $A_{2,9} = 3$ ,  $A_{2,10} = 3$ . Through ii) in Theorem 3 we calculate the reverse upper bounds of  $A_{3l}$  (denoted as  $\tau_l$ ) equal  $\tau_6 = 2.772$ ,  $\tau_7 = 0.1734$ ,  $\tau_8 = 0.1734$ ,  $\tau_9 = 0.5927$ ,  $\tau_{10} = 0.1734$ .

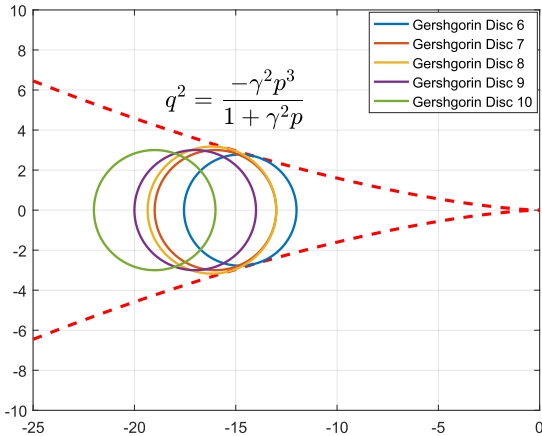


**FIGURE 12.** The Gershgorin discs corresponding to the situation the strength of the reverse edge is in the upper bound. When the strength of reverse edges are lower than the upper bound, the curve  $q^2 = \frac{-\gamma^2 p^3}{1+\gamma^2 p}$  is always separate from all the Gershgorin discs. Note that Gershgorin disc  $i$  (in the reverse range  $i \leq l \leq k$ ) corresponds to the disc for the  $l$ th row in Laplacian matrix  $\mathcal{L}'$ , e.g., Gershgorin disc 6 is for the 6th row.

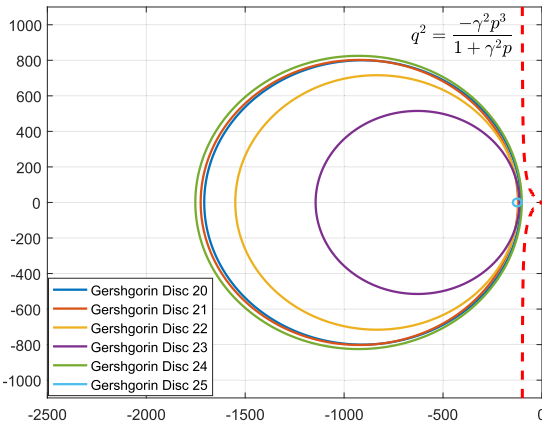


**FIGURE 13.** The Gershgorin discs corresponding to the situation the strength of reverse edges reach sufficient high. When  $A_{1l} > \frac{1}{\gamma^2}$ , the right endpoints of Gershgorin discs are on the left side of  $p = -\frac{1}{\gamma^2}$ , so the curve  $q^2 = \frac{-\gamma^2 p^3}{1+\gamma^2 p}$  is always separate from all the Gershgorin discs even though the radius get sufficiently large.

The corresponding Gershgorin discs are shown in Fig. 12.

In this case  $\max_{2 \leq i \leq N} \frac{q_i}{\sqrt{-p_i}|\mu_i|} = 0.0367 < 0.05$ , and the system can achieve formation stability.

Now we will give an example that when  $A_{1l} > \frac{1}{\gamma^2}$ , i.e., the strengthen of reverse edges can reach infinity. We consider a 30 UAV formation system with  $\gamma = 0.1$ , and the reverse range is from 20 to 25, where  $A_{1,20} = 107, A_{1,21} = 121, A_{1,22} = 118, A_{1,23} = 114, A_{1,24} = 102, A_{1,25} = 103$ , while the reverse edge  $w_{20,25} = 800, w_{21,25} = 800, w_{22,25} = 700, w_{23,25} = 500, w_{24,25} = 800$ . The Gershgorin discs corresponding is shown in Fig. 13. From Fig. 13 we can see the Gershgorin discs have no intersections with the curve  $q^2 = \frac{-\gamma^2 p^3}{1+\gamma^2 p}$ ,  $\gamma_0 = \max_{2 \leq i \leq N} \frac{q_i}{\sqrt{-p_i}|\mu_i|} = 0.0015 < 0.1$ . Thus the system can achieve formation stability.

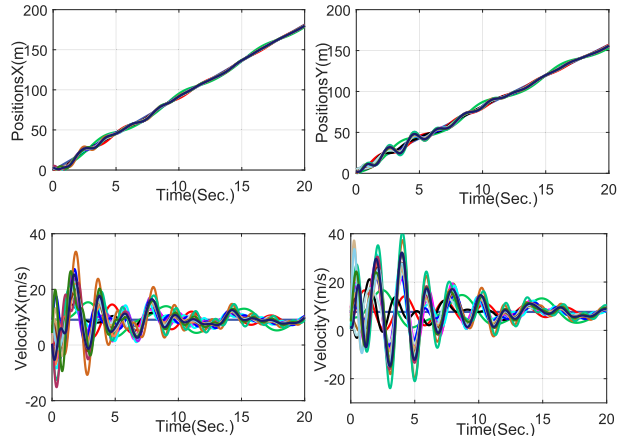


**FIGURE 14.** The position and velocity response of the original system of 20 UAVs before UAVs joining in or quitting from 1 to  $i - 1$ .

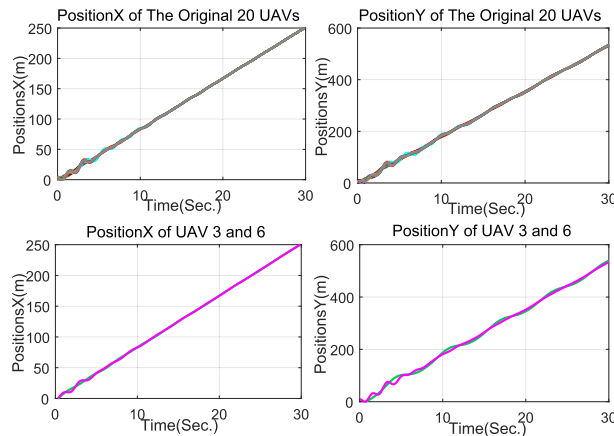
Simulations of the affect of reverse edges on scalability are provided as follows. Consider the original 20 UAVs formation system we mentioned above, whose transformed position response  $\hat{\xi}$  and the velocity response  $\zeta$  are shown in Fig. 14, where  $\gamma = 0.05$ . Now two UAVs with  $Q$  value higher than UAV 6 join in the formation [corresponding to case i) in Remark 4], they are labeled as UAV 3 and UAV 6 after joining the system, and the original UAV 6 becomes UAV 7.

In this case,  $A_{1l}$  increases, and the reverse range turns into from 8 to 12 with  $A_{1,8} = 18, A_{1,9} = 20, A_{1,10} = 19, A_{1,11} = 17, A_{1,12} = 18$ , and the reverse upper bounds  $\tau_l$  also increase to  $\tau_8 = 5.4989, \tau_9 = 3.5896, \tau_{10} = 3.0328, \tau_{11} = 1.988, \tau_{12} = 2.4989$ . Since  $\gamma_0 = 0.0217 < \gamma = 0.05$ , the system achieves formation stability, the transformed position response  $\hat{\xi}$  and the velocity response  $\zeta$  are shown in Fig. 15.

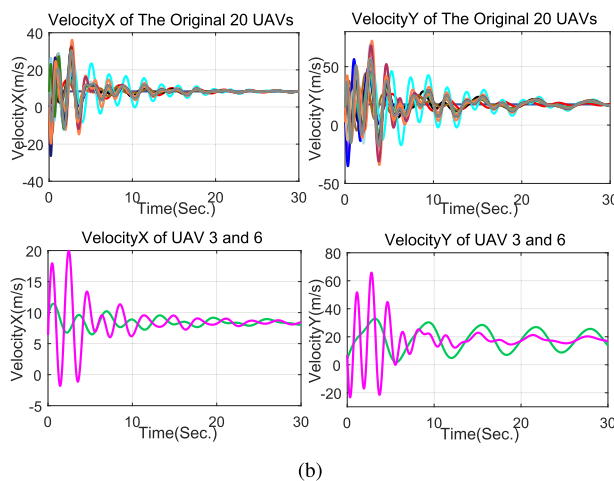
When agents labeled 2, 3, 4 quit the system, the reverse range turns into from 3 to 7,  $A_{1,3} = 6, A_{1,4} = 7, A_{1,5} = 5, A_{1,6} = 3, A_{1,7} = 5$ , and the reverse upper bound  $\tau_l$  decrease,  $\tau_3 = 0.8958, \tau_4 = -1.8915, \tau_5 = -2.3310, \tau_6 = -2.7021, \tau_7 = -2.3310, \gamma_0 = 0.0685 > 0.05$ , by this time the system no longer maintains formation stability, see (Fig. 16).

Next we will give an example of UAVs joining and quitting in the reverse range[corresponding to case ii) in Remark 4]. Consider a 20 UAVs formation system,  $\gamma = 0.05$ , and the reverse range is from 6 to 10.  $A_{1,6} = 15, A_{1,7} = 14, A_{1,8} = 13, A_{1,9} = 15, A_{1,10} = 13$ , while  $A_{2,6} = 0, A_{2,7} = 3, A_{2,8} = 1, A_{2,9} = 3, A_{2,10} = 1$ . The corresponding reverse upper bounds are  $\tau_6 = 4.0349, \tau_7 = 0.5927, \tau_8 = 2.1734, \tau_9 = 1.0349, \tau_{10} = 2.1734$ . When the reverse edges are  $w_{6,10} = 4, w_{8,10} = 2$ , the transformed position response  $\hat{\xi}$  and the velocity response  $\zeta$  of the system are shown in Fig. 17.

When three new UAVs join in the reverse range, they are labeled as 8, 9, 10, and the original UAV 8 becomes UAV 11. The reverse range turns into from 6 to 13.  $A_{1,8} = 7, A_{1,9} = 7, A_{1,10} = 6$ , and  $A_{2,9} = 9, A_{2,10} = 11, A_{2,11} = 11, A_{2,12} = 12, A_{2,13} = 6$ . The reverse upper bounds are  $\tau_6 = 4.0349, \tau_7 = 0.5927, \tau_8 = -7.8515, \tau_9 = -7.8515, \tau_{10} = -10.1042, \tau_{11} = -7.8266, \tau_{12} = -7.9651, \tau_{13} = -2.8266$ .



(a)



(b)

**FIGURE 15.** Two new UAVs labeled 3 and 6 join in the system. For each  $l$  in the reverse range,  $A_{1l}$  increases, so the upper bound also increases, the coupling strength of reverse edges do not exceed, hence the formation maintains its pattern. (a) Position response of the system; (b) Velocity response of the system.

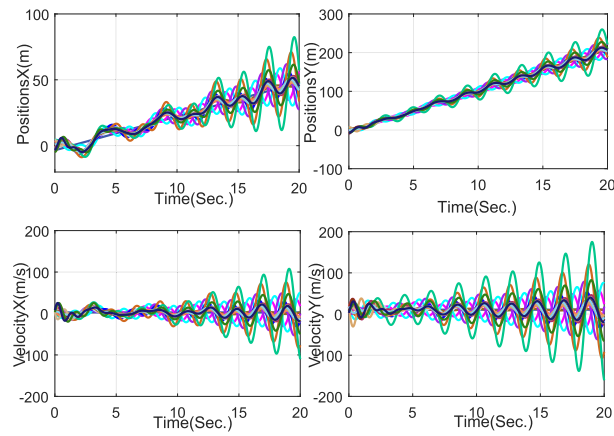


**FIGURE 16.** When UAV 2, 3, 4 quit the formation, for each  $l$  in the reverse edge, as  $A_{1l}$  decreases, the reverse upper bound also decreases. The coupling strength of reverse edges exceed the upper bounds and the system no longer maintains stable.

Since  $\gamma_0 = 0.0518 > \gamma = 0.05$ , the system cannot maintain stability, and the transformed position response  $\hat{\xi}$  and the velocity response  $\zeta$  are shown in Fig. 18.

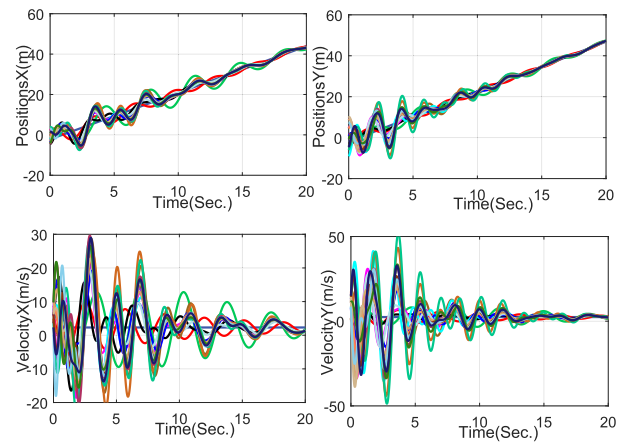
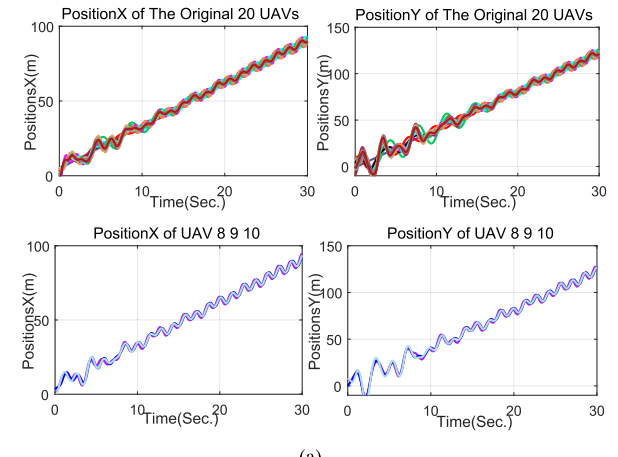
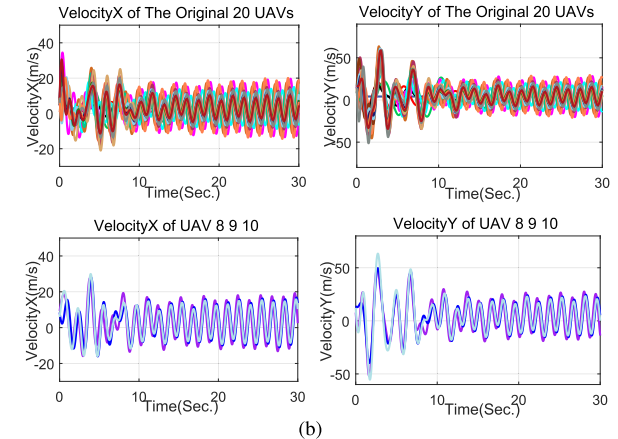


**FIGURE 17.** The position and velocity response of the original system of 20 UAVs before UAV joining or quitting the formation. To show the existence of reverse edges may affect the scalability of system, there are two reverse edges in the topology, their coupling strength are lower than the upper bound given by Theorem 3.



(a)



(b)

**FIGURE 18.** Three new UAVs labeled 8, 9, 10 join in the reverse range. For each  $l$  in the reverse range, as  $A_{2l}$  increases, the reverse upper bound of the system decreases. As a result, the coupling strength of reverse edges exceed the upper bound, and thus the system is no longer stable. (a) Position response of the system; (b) Velocity response of the system.

When two UAVs labeled 8 and 9 quit from the original 20 UAV formation system, the reverse range is from 6 to 8 with  $A_{2,6} = 0$ ,  $A_{2,7} = 1$ ,  $A_{2,8} = 1$ . The reverse upper

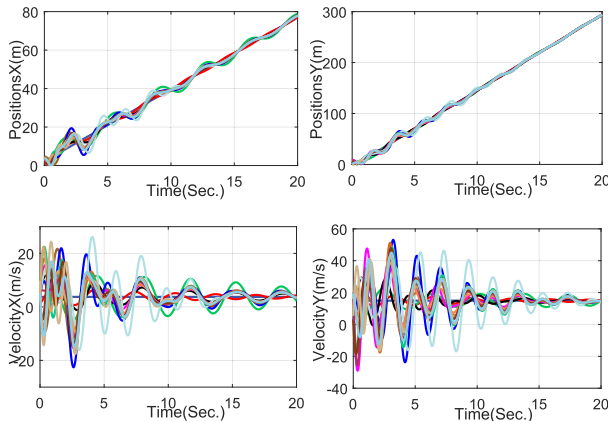


**FIGURE 19.** UAV 8 and 9 quit the formation, for each  $l$  in the reverse range, as  $A_{2l}$  decreases, the reverse upper bound increases and the system still achieves formation stability.

bounds are  $\tau_6 = 4.0349$ ,  $\tau_7 = 3.0349$ ,  $\tau_8 = 2.1734$ . Since  $\gamma_0 = 0 < \gamma = 0.05$ , the system achieves formation stability (see Fig. 19).

## VII. CONCLUSION

In this paper, the scalability problem has been studied for UAV formation control with double-integrator dynamics. Inspired from pigeon flocks, we have proposed the Veteran Rule to solve this problem under fixed control parameters. Furthermore, the convergence rate of the formation system under the proposed Veteran Rule has been analyzed. Counterintuitively, we found that the optimal convergence rate requires all the in-degrees to equal  $\frac{4}{\gamma^2}$ , where  $\gamma$  is the control parameter; and any additional in-degrees do not contribute to the convergence rate, but have negative effects. Based on this result, the Veteran Rule with optimal convergence rate has been designed. An upper bound of reverse edges in a given reverse range has been proposed to guarantee the formation stability, and the effect of reverse edges of the system were analyzed in three different cases. Simulation results have shown the effectiveness of our theory and design.

### Future Work

For future work, we are going to explore the propagation of uncertainty in the system topology, we analyze how a small error or the noise in the state of an agent affects other agents' states, and how to reduce uncertainties in a network topology utilizing filtering theories [38], [39]. Moreover, fuzzy model of multi-UAV formation systems [40] and some analysis of the key nodes of the network topology [41] will be considered.

## REFERENCES

- [1] X. Dong, B. Yu, Z. Shi, and Y. Zhong, "Time-varying formation control for unmanned aerial vehicles: Theories and applications," *IEEE Trans. Control Syst. Technol.*, vol. 23, no. 1, pp. 340–348, Jan. 2015.
- [2] J. Han, Y. Xu, L. Di, and Y. Chen, "Low-cost Multi-UAV technologies for contour mapping of nuclear radiation field," *J. Intell. Robotic Syst.*, vol. 70, pp. 401–410, Apr. 2013.
- [3] B. D. O. Anderson, B. Fidan, C. Yu, and D. Walle, "UAV formation control: Theory and application," in *Recent Advances in Learning and Control*. V. D. Blondel, S. P. Boyd, and H. Kimura, Eds., London, U.K.: Springer, 2008, pp. 15–33.
- [4] D. Luo, W. Xu, S. Wu, and Y. Ma, "UAV formation flight control and formation switch strategy," in *Proc. 8th Int. Conf. Comput. Sci. Educ.*, Apr. 2013, pp. 264–269.
- [5] Y. Cao, W. Yu, W. Ren, and G. Chen, "An overview of recent progress in the study of distributed multi-agent coordination," *IEEE Trans. Ind. Informat.*, vol. 9, no. 1, pp. 427–438, Feb. 2013.
- [6] X. Wang, Z. Zeng, and Y. Cong, "Multi-agent distributed coordination control: Developments and directions via graph viewpoint," *Neurocomputing*, vol. 199, pp. 204–218, Jul. 2016.
- [7] Z. Li, Z. Duan, G. Chen, and L. Huang, "Consensus of multiagent systems and synchronization of complex networks: A unified viewpoint," *IEEE Trans. Circuits Syst. I, Reg. Papers*, vol. 57, no. 1, pp. 213–224, Jan. 2010.
- [8] Z. Li, G. Wen, Z. Duan, and W. Ren, "Designing fully distributed consensus protocols for linear multi-agent systems with directed graphs," *IEEE Trans. Autom. Control*, vol. 60, no. 4, pp. 1152–1157, Apr. 2015.
- [9] F. Muñoz, E. S. E. Quesada, H. M. La, S. Salazar, S. Commuri, and L. R. G. Carrillo, "Adaptive consensus algorithms for real-time operation of multi-agent systems affected by switching network events," *Int. J. Robust Nonlinear Control*, vol. 27, no. 9, pp. 1566–1588, 2017.
- [10] W. Yu, W. X. Zheng, J. Lü, and G. Chen, "Designing distributed control gains for consensus in multi-agent systems with second-order nonlinear dynamics," *IFAC Proc. Volumes*, vol. 44, no. 1, pp. 1231–1236, Jan. 2011.
- [11] C. W. Reynolds, "Flocks, herds, and schools: A distributed behavioral model," *Comput. Graph.*, vol. 21, no. 4, pp. 25–34, Jul. 1987.
- [12] T. Vicsek, A. Czirók, E. Ben-Jacob, I. Cohen, and O. Shochet, "Novel type of phase transition in a system of self-driven particles," *Phys. Rev. Lett.*, vol. 75, no. 6, p. 1226, Aug. 1995.
- [13] W. Ren and R. W. Beard, "Consensus seeking in multiagent systems under dynamically changing interaction topologies," *IEEE Trans. Autom. Control*, vol. 50, no. 5, pp. 655–661, May 2005.
- [14] W. Ren, "On consensus algorithms for double-integrator dynamics," *IEEE Trans. Autom. Control*, vol. 53, no. 6, pp. 1503–1509, Jul. 2008.
- [15] L. Cheng, Z.-G. Hou, M. Tan, and X. Wang, "Necessary and sufficient conditions for consensus of double-integrator multi-agent systems with measurement noises," *IEEE Trans. Autom. Control*, vol. 56, no. 8, pp. 1958–1963, Apr. 2011.
- [16] J. Zhu, Y.-P. Tian, and J. Kuang, "On the general consensus protocol of multi-agent systems with double-integrator dynamics," *Linear Algebra Appl.*, vol. 431, pp. 701–715, Aug. 2009.
- [17] X. Wang and Y. Hong, "Finite-time consensus for multi-agent networks with second-order agent dynamics," *IFAC Proc. Volumes*, vol. 41, no. 2, pp. 15185–15190, 2008.
- [18] Y. Cao, W. Ren, and Z. Meng, "Decentralized finite-time sliding mode estimators and their applications in decentralized finite-time formation tracking," *Syst. Control Lett.*, vol. 59, no. 9, pp. 522–529, Sep. 2010.
- [19] J. Xi, N. Cai, and Y. Zhong, "Consensus problems for high-order linear time-invariant swarm systems," *Phys. A, Stat. Mech. Appl.*, vol. 389, no. 24, pp. 5619–5627, Dec. 2010.
- [20] Z. Li, Z. Duan, and G. Chen, "Dynamic consensus of linear multi-agent systems," *IET Control Theory Appl.*, vol. 5, no. 1, pp. 19–28, Jan. 2011.
- [21] J. Qin and C. Yu, "Cluster consensus control of generic linear multi-agent systems under directed topology with acyclic partition," *Automatica*, vol. 49, no. 9, pp. 2898–2905, Sep. 2013.
- [22] Z. Li, W. Ren, X. Liu, and L. Xie, "Distributed consensus of linear multi-agent systems with adaptive dynamic protocols," *Automatica*, vol. 49, no. 7, pp. 1986–1995, 2013.
- [23] Z. Li, W. Ren, X. Liu, and M. Fu, "Consensus of multi-agent systems with general linear and Lipschitz nonlinear dynamics using distributed adaptive protocols," *IEEE Trans. Autom. Control*, vol. 58, no. 7, pp. 1786–1791, Jul. 2013.
- [24] W. Yu, W. Ren, W. X. Zheng, G. Chen, and J. Lü, "Distributed control gains design for consensus in multi-agent systems with second-order nonlinear dynamics," *Automatica*, vol. 49, no. 7, pp. 2107–2115, Jul. 2013.
- [25] H. Yu and X. Xia, "Adaptive consensus of multi-agents in networks with jointly connected topologies," *Automatica*, vol. 48, no. 8, pp. 1783–1790, Aug. 2012.

- [26] J. Sun, Z. Geng, Y. Lv, Z. Li, and Z. Ding, "Distributed adaptive consensus disturbance rejection for multi-agent systems on directed graphs," *IEEE Trans. Control Netw. Syst.*, vol. 5, no. 1, pp. 629–639, Mar. 2018.
- [27] M. Nagy, Z. Ákos, D. Biro, and T. Vicsek, "Hierarchical group dynamics in pigeon flocks," *Nature*, vol. 464, no. 7290, pp. 890–893, Apr. 2010.
- [28] H. E. Bell, "Gershgorin's theorem and the zeros of polynomials," *Amer. Math. Monthly*, vol. 72, no. 3, pp. 292–295, 1965.
- [29] J. Bang-Jensen and G. Gutin, *Digraphs Theory, Algorithms and Applications*, ser. Monographs in Mathematics. Springer, 2001.
- [30] H.-T. Zhang, Z. Chen, and X. Mo, "Effect of adding edges to consensus networks with directed acyclic graphs," *IEEE Trans. Autom. Control*, vol. 62, no. 9, pp. 4891–4897, Sep. 2017.
- [31] R. Olfati-Saber and R. M. Murray, "Consensus problems in networks of agents with switching topology and time-delays," *IEEE Trans. Autom. Control*, vol. 49, no. 9, pp. 1520–1533, Sep. 2004.
- [32] M. Vidyasagar, *Nonlinear Systems Analysis*, vol. 42. Philadelphia, PA, USA: SIAM, 2002.
- [33] W. Yu, G. Chen, and M. Cao, "Some necessary and sufficient conditions for second-order consensus in multi-agent dynamical systems," *Automatica*, vol. 46, no. 6, pp. 1089–1095, 2010.
- [34] I. Watts, B. Pettit, M. Nagy, T. B. de Perera, and D. Biro, "Lack of experience-based stratification in homing pigeon leadership hierarchies," *Roy. Soc. Open Sci.*, vol. 3, no. 1, Jan. 2016, Art. no. 150518.
- [35] B. Pettit, Z. Ákos, T. Vicsek, and D. Biro, "Speed determines leadership and leadership determines learning during pigeon flocking," *Current Biol.*, vol. 25, no. 23, pp. 3132–3137, Dec. 2015.
- [36] P. E. Jorge and P. A. M. Marques, "Decision-making in pigeon flocks: A democratic view of leadership," *J. Exp. Biol.*, vol. 215, no. 14, pp. 2414–2417, Jun. 2012.
- [37] C. D. Santos, S. Neupert, H.-P. Lipp, M. Wikelski, and D. K. N. Dechmann, "Temporal and contextual consistency of leadership in homing pigeon flocks," *PLoS ONE*, vol. 9, no. 7, Jul. 2014, Art. no. e102771.
- [38] S. Li, L. Li, Z. Li, X. Chen, T. Fernando, H. H.-C. Iu, G. He, Q. Wang, and X. Liu, "Event-trigger heterogeneous nonlinear filter for wide-area measurement systems in power grid," *IEEE Trans. Smart Grid*, vol. 10, no. 3, pp. 2752–2764, May 2019.
- [39] X. Liu, L. Li, Z. Li, X. Chen, T. Fernando, H. H.-C. Iu, and G. He, "Event-trigger particle filter for smart grids with limited communication bandwidth infrastructure," *IEEE Trans. Smart Grid*, vol. 9, no. 6, pp. 6918–6928, Nov. 2018.
- [40] Y. Yu, Z. Li, X. Liu, K. Hirota, X. Chen, T. Fernando, and H. H.-C. Iu, "A nested tensor product model transformation," *IEEE Trans. Fuzzy Syst.*, vol. 27, no. 1, pp. 1–15, Jan. 2019.
- [41] B. Liu, Z. Li, X. Chen, Y. Huang, and X. Liu, "Recognition and vulnerability analysis of key nodes in power grid based on complex network centrality," *IEEE Trans. Circuits Syst. II, Exp. Briefs*, vol. 65, no. 3, pp. 346–350, Mar. 2018.



**YU DING** received the bachelor's degree in automation from the Harbin Institute of Technology, Harbin, China, in 2017. He is currently pursuing the M.S. degree in control science and engineering with the National University of Defense Technology. His current research interests include formation control, multi-agent systems, and filtering theory.



**XIANGKE WANG** (M'12–SM'18) received the B.S., M.S., and Ph.D. degrees in control science and engineering from the National University of Defense Technology, Changsha, China, in 2004, 2006, and 2012, respectively.

Since 2014, he has been an Associate Professor with the College of Mechatronic Engineering and Automation, National University of Defense Technology. He has published a number of journal articles. His current research interests include coordinated decision and control of multiple unmanned aerial vehicle (UAV) systems, nonlinear control, and visual servo control.



**YIRUI CONG** (S'14–M'18) received the B.E. degree (Hons.) in automation from Northeastern University, Shenyang, China, in 2011, the M.Sc. degree (graduated in advance) in control science and engineering from the National University of Defense Technology, Changsha, China, in 2013, and the Ph.D. degree from Australasian National University, Canberra, ACT, Australia, in 2018. He is currently a Lecturer with the National University of Defense Technology. His research interests include communication theory and control theory.



**HUIMING LI** received the bachelor's degree in automation from Northeastern University, Shenyang, China, in 2018. She is currently pursuing the master's degree in control science and engineering with the National University of Defense Technology. Her current research interests include formation control and multi-agent systems.

• • •